PERGAMON

Electrochimica Acta 47 (2002) 1359–1364

ELECTROCHIMICA Acta

www.elsevier.com/locate/electacta

In vitro corrosion behaviour of titanium alloys without vanadium

M.F. López [a,*], A. Gutiérrez [b], J.A. Jiménez [c]

[a] *Instituto de Ciencia de Materiales de Madrid, CSIC, Cantoblanco, E-28049 Madrid, Spain*
[b] *Departamento de Ciencia y Tecnología de Materiales, Universidad Miguel Hernández, Avda Ferrocarril s/n, E-03202 Elche, Spain*
[c] *Centro Nacional de Investigaciones Metalúrgicas, CSIC, Avda Gregorio del Amo 8, E-28040, Spain*

Received 5 June 2001; received in revised form 18 October 2001

Abstract

The corrosion behaviour of three new non-toxic titanium alloys for use as biomaterials has been investigated. The corrosion current densities of these Ti alloys have low values, indicating a passive state that is stable with time. These values were calculated by using both direct and alternate current methods. The comparison with Ti–6Al–4V, widely used as biomaterial, shows slightly lower corrosion rates for the non V-containing alloys. To determine the pitting corrosion resistance, anodic polarisation curves were performed. Those alloys containing Zr, with very low passivation current densities, show the best behaviour. This indicates a low susceptibility to localised corrosion in these alloys. The chemical surface analysis performed on the samples suggests an influence of the passive layer composition on the passivation current density.

Keywords: Electrochemical techniques; Corrosion; Biomaterials; Ti alloys; Surfaces

1. Introduction

In the field of biomedical materials, metallic biomaterials present clear advantages such as good processability, weldability, satisfactory mechanical properties, etc. [1–3]. However, the main inconvenience of metallic biomaterials is their degradation upon interaction with body fluids [4–6]. This is the reason why materials for conventional metallic implants are selected according to their corrosion resistance, i.e. their capacity to generate a protective passive film. Commercially pure titanium, Ti–6Al–4V alloy, cobalt–chromium alloys and a small number of stainless steels are widely used in biomedical applications. These materials are protected by an external oxide layer, which ensures a satisfactory corrosion resistance. The problem of corrosion is associated with the problem of ion release of metallic species, which can be harmful for the organism. The protective effect of the passive layer not only reduces the corrosion rates of the material, but also ion release [7,8]. The satisfactory corrosion behaviour of pure Ti is due to the TiO_2 layer formed on its surface. However, for a metallic biomaterial, it is essential to have excellent mechanical properties too. In general, Ti alloys exceed the mechanical properties of pure Ti [9,10]. Thus, Ti–6Al–4V alloy has been widely investigated [11–14], becoming one of the major alloys used for manufacture of orthopaedic implants. However, due to tissular reaction, vanadium has been classified as one of the elements of the toxic group [15,16]. The possibility of V ion release makes essential the development of Ti alloys without V in their composition with satisfactory properties for biomedical applications.

As mentioned above, one determining factor for the success of new alloys as biomaterials is their corrosion behaviour. Therefore, the in vitro evaluation of their corrosion parameters is one of the first steps in the development of new biomaterials. Additionally, the corrosion behaviour of a material strongly depends on the presence of a protective passive film, i.e. is mainly a surface phenomenon. Consequently, the determination of the passive film composition complements the in vitro corrosion evaluation. The characterisation of the surface composition is of high interest also because most external layers of a biomaterial will be in direct contact with biological tissues.

In this work, the corrosion behaviour of three non V-containing Ti alloys, Ti–7Nb–6Al, Ti–13Nb–13Zr and Ti–15Zr–4Nb, by means of electrochemical tech-

* Corresponding author. Fax: +34-913720623.
E-mail address: mflopez@icmm.csic.es (M.F. López).

0013-4686/02/$ - see front matter
PII: S0013-4686(01)00860-X

niques was evaluated. The passive film composition of the three alloys as well as its role on their corrosion behaviour was investigated by performing X-ray photoelectron spectroscopy (XPS).

2. Experimental

Three Ti basis alloys were prepared by arc melting and then casting in a copper coquille under high vacuum. The chemical compositions of these alloys were (in wt.%); Ti–7Nb–6Al, Ti–13Nb–13Zr and Ti–15Zr–4Nb. In order to obtain a two phase ($\alpha+\beta$) microstructure, which ensures satisfactory mechanical properties, the same annealing procedure was conducted on all samples. The alloys were annealed above the β-transition temperature at 1100 °C for 1 h and subsequently aged at 700 °C for 1 h. The microstructures of the three Ti alloys after this treatment were characterised using various techniques including optical microscopy, and scanning electron microscopy (SEM) equipped with energy dispersive X-ray microanalysis (EDX). Metallographic preparation included mounting the samples in bakelite and polishing by the conventional method.

The corrosion behaviour of the Ti alloys was evaluated at room temperature using as electrolyte an aerated solution, the Hank's solution, with pH 7.4. The chemical composition of this solution is 8 g/l NaCl, 1 g/l glucose, 0.4 g/l KCl, 0.35 g/l $NaHCO_3$, 0.14 g/l $CaCl_2$, 0.1 g/l $MgCl_2 \cdot 6H_2O$, 0.06 g/l $Na_2HPO_4 \cdot 2H_2O$, 0.06 g/l KH_2PO_4 and 0.06 g/l $MgSO_4 \cdot 7H_2O$. The Hank's solution is commonly used for in vitro corrosion studies in biomaterials because it simulates the physiological media of the human body. Before testing, the Ti alloys samples were abraded and polished using diamond paste with particle size ranging from 9 to 1 μm. Colloidal silica was used as last step of polishing to ensure a surface free of mechanical deformation. Finally, the samples were ultrasonically degreased in acetone. An area of 3.46 cm^2 for all samples, as working electrodes, was immersed in the Hank's solution. A saturated calomel electrode was used as a reference electrode and a platinum wire as counter electrode. The electrochemical techniques used to evaluate the corrosion behaviour of all samples were the following;

1. Evolution of the corrosion potential, *E*corr, with testing time.
2. Determination of the Tafel polarisation curves up to ± 0.250 V at a scanning rate of 60 mV/min to calculate the anodic and cathodic slopes, β_a and β_c, respectively. Taking into account the equation $B = \beta_a \times \beta_b/[2.3(\beta_a+\beta_b)]$, the value of the constant B can be deduced. This constant is essential to evaluate the corrosion rate [17].
3. Linear polarisation. In order to use this method, potential steps of 10 mV were applied and the intensity ΔI was registered. The value of the anodic polarisation resistance, R_p, was deduced from the equation $R_p = \Delta E/\Delta I$, where ΔE is the step of the potential applied at the corrosion potential and ΔI is the resulting current for a testing time of 60 s. After determining the polarisation resistance, the corrosion current densities, i_{corr}, can be calculated by applying the Stern–Geary equation [17] ($i_{corr} = B/R_p$), where the value of B was previously obtained.
4. Electrochemical impedance spectroscopy (EIS) measurements. For these experiments a sinusoidal potential variation with 10 mV amplitude was applied within a frequency range from 0.001 to 64 000 Hz.
5. Determination of the anodic polarisation curves at a scanning rate of 10 mV/min to evaluate the pitting corrosion susceptibility.

The chemical composition of the passive layer of the different materials was studied by X-ray photoemission spectroscopy (XPS). XPS spectra were recorded under ultra-high vacuum (UHV) conditions with a VG-CLAM hemispherical electron energy analyser using Mg X-rays as excitation source. The base pressure in the UHV chamber during measurements was better than 10^{-9} mbar. Samples were cleaned by sputtering with an ion gun operating at a sample current of 1 μA, an ion energy of 5 keV and a sputter rate of approximately 10 Å/min.

3. Results and discussion

Fig. 1 represents the SEM micrographs of the three Ti alloys. All of them exhibit a coarse microstructure with two phases. Ti–7Nb–6Al and Ti–15Zr–4Nb alloys, Fig. 1a and c, respectively, show platelike grains surrounded by a lighter intergranular phase. As the size of this lighter phase is smaller than the excitation area of the electron beam, only a qualitative analysis by EDX was possible. This microanalysis shows a high level of Nb in the light phase, as well as a negligible amount of Nb in the dark phase. For the case of Ti–13Nb–13Zr, since the lighter regions are larger, it was possible to perform quantitative microanalysis. Thus, the EDX spectrum in Ti–13Nb–13Zr reveals a content of 21% of Nb in the light phase, while in the dark phase no Nb emission could be detected. As Nb stabilises the β phase, this result indicates that the light phase corresponds to the β phase. The Ti–13Nb–13Zr sample is richer in β phase (lighter region) than Ti–7Nb–6Al and Ti–15Zr–4Nb alloys, as observed in Fig. 1c. This result was expected because the chemical composition of Ti–13Nb–13Zr includes a higher amount of the β-stabiliser Nb.

The anodic and cathodic polarisation curves were measured to calculate the Tafel slopes, β_a and β_c. Table 1 shows the β_a, β_c and B values obtained after 37 days of immersion in Hank's solution. The B values obtained are quite similar for all samples and are typical of materials in a passive state.

Additionally, the E_{corr} values were measured during 35 days of immersion in the electrolyte and were almost constant for each titanium alloy. The average E_{corr} values were 175, −72 and 127 mV for Ti–7Nb–6Al, Ti–13Nb–13Zr and Ti–15Zr–4Nb, respectively. These values did not change appreciably during the testing time. Again, this result is representative of materials in a passive state.

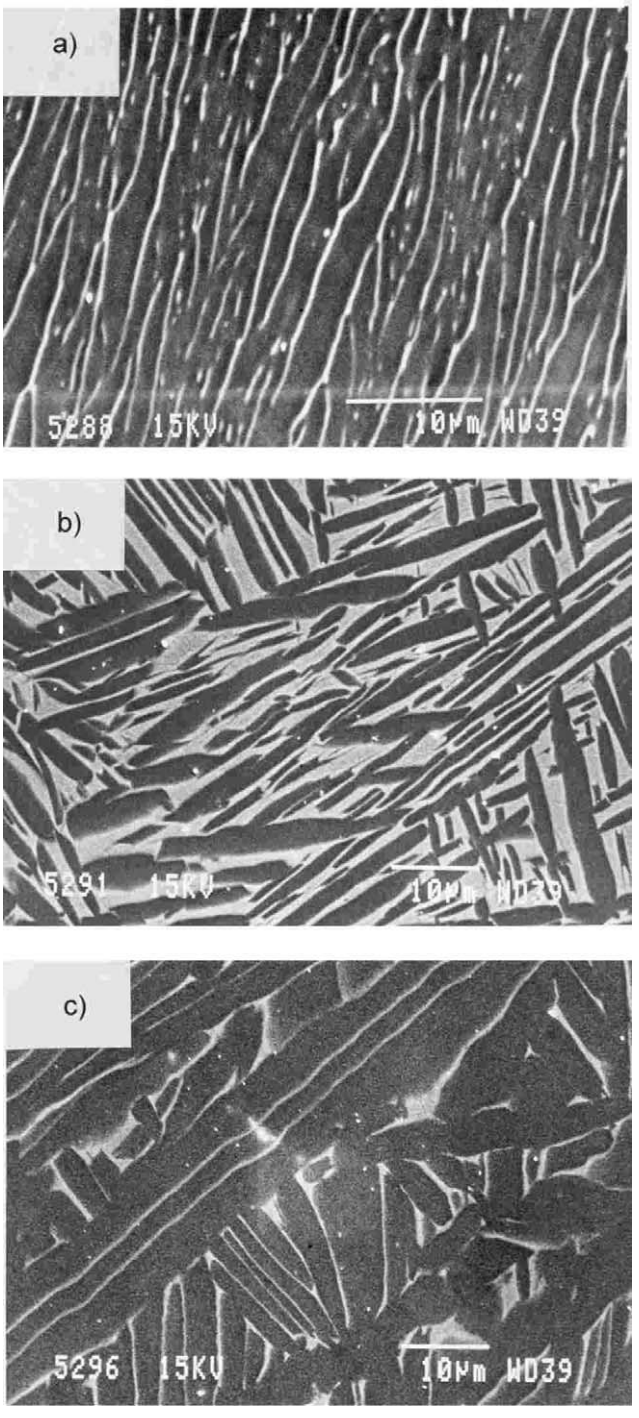

Fig. 1. SEM micrographs of (a) Ti–7Nb–6Al; (b) Ti–13Nb–13Zr; and (c) Ti–15Zr–4Nb.

Table 1
β_a, β_c, and B values obtained from the anodic and cathodic Tafel polarisation curves for the three Ti alloys immersed in Hank's solution

Material	β_a (mV)	β_c (mV)	B (mV)
Ti–7Nb–6Al	740	118	44
Ti–13Nb–13Zr	577	200	64
Ti–15Zr–4Nb	375	141	44

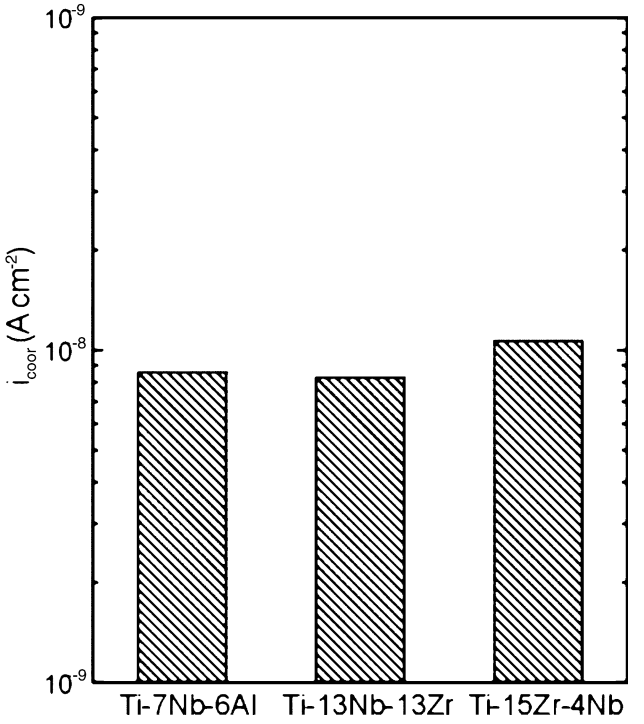

Fig. 2. Average values of corrosion current densities, i_{corr} for the three Ti alloys during 35 days of immersion in Hank's solution as calculated by using the polarisation resistance method.

In Fig. 2, average values of the corrosion current density, i_{corr}, throughout 35 days of immersion in Hank's solution are represented for the three Ti alloys. To obtain these values, first the polarisation resistance method was used to get the R_p values. Then by means of the Stern–Geary equation using the B values obtained from the Tafel slopes and the R_p data, the i_{corr} values were calculated. As it can be observed, the corrosion current densities for all three Ti alloys are very similar. These values are slightly lower than the corrosion current density obtained in previous works for the Ti–6Al–4V alloy, which was around 5×10^{-8}

A/cm^2 [18]. This result indicates that the corrosion behaviour for these new Ti alloys is at least as good as that of Ti–6Al–4V. The corrosion resistance can also be obtained by means of the impedance method, also known as EIS. To verify the corrosion data obtained by the polarisation resistance method, EIS experiments were also carried out. In the EIS measurements, the modulus of the impedance, $|Z|$ versus the frequency is registered. The transfer resistance, R_T, can be approximated to the $|Z|$ value corresponding to the lowest frequency. This value of the transfer resistance, R_T, can be associated, in most cases, to the R_P value determined by the polarisation resistance method [4]. Therefore, taking into account the R_T values obtained by EIS, the B values from Table 1, and applying the Stern–Geary equation, corrosion current density values can be estimated from EIS data. Fig. 3 represents the variation of i_{corr} versus testing time for the different Ti alloys from the EIS experiments. It can be seen that i_{corr} for the three Ti alloys have a large decrease during the first days of immersion in Hank's solution and become almost constant with testing time after this decrease. This behaviour is representative of materials in a passive state. As can be observed in Fig. 3, the i_{corr} values reached after the first day of immersion in the electrolyte are rather low. These low i_{corr} values are due to the presence of a passive layer on the material surface that protects it from the aggressive environment. From Fig. 3, it can be deduced that this layer is very stable with time giving a high corrosion resistance to the three Ti alloys.

As can be seen by comparing Figs. 2 and 3, the average i_{corr} values obtained by EIS (alternate current) are of the same order of magnitude that those obtained by the polarisation resistance method (direct current). These values are quite low ($\approx 10^{-8}$ A/cm^2), even lower than those obtained for conventional biomaterials investigated in previous studies, like Co–Ni–Cr and Ti–Al–V alloys [18]. These low i_{corr} values observed for the three Ti alloys suggest an excellent resistance against uniform corrosion.

In addition to uniform corrosion, materials exposed to an aggressive environment can undergo local corrosion, in which the passive layer breaks down locally leading to the formation of pits. In the case of biomaterials, this kind of failure can take place under special conditions such as local infections, surgical trauma, etc. Therefore, it is very important to evaluate the susceptibility to pitting corrosion of these materials, which can be determined by means of cyclic anodic polarisation curves. Although, the resistance to uniform corrosion of the three alloys is similar, the resistance to pitting

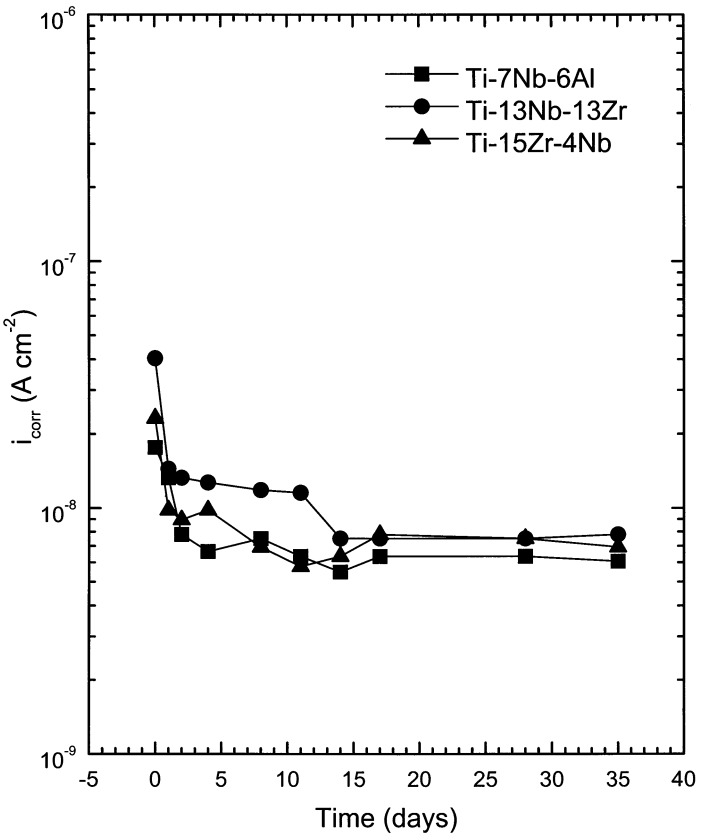

Fig. 3. Corrosion current densities, i_{corr} versus testing time for the three different Ti alloys in Hank's solution as deduced from the electrochemical impedance spectroscopy (EIS).

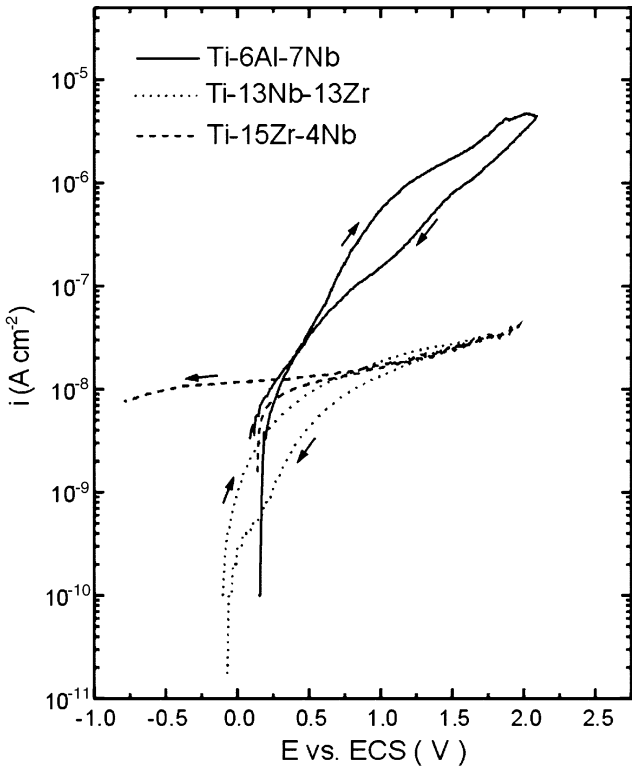

Fig. 4. Anodic polarisation curves at 10 mV/min for the three Ti alloys after 42 days of immersion in Hank's solution.

corrosion can vary depending on the nature of the passive layer. Fig. 4 represents the anodic cyclic polarisation curves of all three Ti alloys after 42 days of immersion in Hank's solution. The main parameters that can be obtained from the anodic polarisation curves are the corrosion potential, E_{corr} the breakdown potential, E_b, and the passivation current density, i_p. For Ti–7Nb–6Al the polarisation curve starts at the E_{corr} value, 0.157 V, the maximum potential range reached was 2.100 V and the minimum was 0.087 V. For Ti–13Nb–13Zr, the curve exhibits an E_{corr} value of -0.101 V, a maximum potential range of 1.670 V and a minimum potential range of -0.071 V. And finally, for Ti–15Zr–4Nb, the E_{corr} value is 0.138 V and the maximum and the minimum potential ranges are 1.970 and -0.800 V, respectively. The breakdown potential corresponds to the local break of the passive layer and gives rise to a sharp increase of the current density. Despite the high voltages probed (up to 2 V), no breakdown is reached in any of the polarisation curves. Ti–7Nb–6Al sample shows the highest values of the current density, which continuously increases by increasing the voltage. However, no sharp enhancement is observed, which would be typical of the appearance of the breakdown potential and, therefore, of the activation of a local corrosion process. This behaviour suggests that the only surface degradation which takes place is uniform corrosion and not pitting corrosion remaining the material in its passive state. The polarisation curves for Ti–13Nb–13Zr and Ti–15Zr–4Nb show a wide passivation region, with very low passivation current densities, around 10^{-8} A/cm^2 in both cases. These values are lower than those of the Ti–7Nb–6Al sample, without any sharp intensity enhancement typical of a localised corrosion process. Therefore, these materials exhibit an excellent resistance to pitting corrosion.

It is interesting to compare the anodic polarisation curves of Fig. 4 with that performed on Ti–6Al–4V in a similar experiment [18]. This comparison shows similar curve shapes with passivation current densities clearly lower for the Ti–13Nb–13Zr and Ti–15Zr–4Nb samples, around 10^{-8} A/cm^2, than for Ti–6Al–4V, between 10^{-6} and 10^{-5} A/cm^2. This suggests a much better corrosion behaviour for these two Ti alloys than for the conventional biomaterial Ti–6Al–4V. With regard to the Ti–7Nb–6Al alloy, it shows current density values from 10^{-8} to 4×10^{-6}, which are slightly lower than the conventional Ti–6Al–4V. These values are higher than those of Ti–13Nb–13Zr and Ti–15Zr–4Nb samples but lower than those of the conventional Ti–6Al–4V alloy As in the three studied Ti alloys, no breakdown potential was observed for Ti–6Al–4V in ref. [18], indicating a very low probability of formation of pits in all cases. The results on the three Ti alloys under study can be also compared with other conventional biomaterials such as Co alloys or coated stainless steels where a clear breakdown potential was found after 0.5 V of polarisation [18].

The different corrosion behaviour of materials is related to the properties of their passive layer and, in particular, to its composition. In order to better understand the observed differences between the three alloys investigated, a surface analysis was performed by XPS. The XPS spectra revealed for the three Ti alloys a passive layer formed by a mixture of Ti, Al or Zr, and, in less proportion, Nb oxides [19]. Table 2 shows in atomic % (at.%), the surface composition of the three alloys, the bulk composition and the ratio between both values. The surface composition was calculated from the XPS data. More details about spectral analysis can be found elsewhere [19]. The bulk atomic percentage values are known from the chemical composition of the material. The ratio between surface and bulk composition gives an estimation of the diffusion of the alloying elements from the bulk region to the surface to form the passive layer. As can be observed, for all samples the Ti and Nb content at the surface decrease with respect to the bulk, indicating no preferential diffusion of these elements towards the surface. On the other hand, the Al and Zr content strongly increases from bulk to surface, showing a clear diffusion of these elements towards the surface of the material to form the passive layer. The Al content at the surface of

Table 2
Surface and bulk atomic percentage values of the different alloying elements of the three Ti alloys, and the ratio between both values

Material	Alloying element	Surface (at.%)	Bulk (at.%)	Ratio surface/bulk
Ti–7Nb–6Al				
	Ti	69.2	86	0.80
	Nb	2.9	3.5	0.83
	Al	27.9	10.5	2.65
	Ti	55.9	84.5	0.66
Ti–13Nb–13Zr				
	Nb	5.1	7.7	0.66
	Zr	39	7.8	5.01
	Ti	57.3	89.1	0.64
Ti–15Zr–4Nb				
	Zr	40.9	8.6	4.73
	Nb	1.8	2.3	0.78

Ti–7Nb–6Al is almost three times that in the bulk, whereas in the case of Zr, both in Ti–13Nb–13Zr and Ti–15Zr–4Nb, the ratio surface/bulk is even higher. This suggests a relative higher amount of Zr in the passive layer of Zr-containing alloys (39 and 40.9 at.%) than Al in the passive layer of the Al-containing alloy (27.9 at.%). One can relate this result to the different current density values obtained in the anodic curves between the Zr-containing and the Al-containing Ti alloys. Elemental Al and Zr have both a tendency to form very protective passive layers. The higher concentration of Zr in the passive layer of the Zr-containing alloys, as compared with the Al concentration in the passive layer of Ti–7Nb–6Al, can explain the lower current densities observed in the first case. Additional effects associated with chemical and structural differences between Al- and Zr-containing passive layers cannot be excluded.

4. Conclusions

The corrosion behaviour of three new titanium alloys not containing V developed for biomedical applications has been investigated by means of electrochemical techniques and surface analysis. The corrosion rates of these Ti alloys are very low compared with conventional biomaterials. The corrosion current densities are also very stable with time, indicating a passive state. The probability of breakdown of the protective passive film is also studied by means of anodic polarisation curves. The lowest passivation current density values correspond to Ti–13Nb–13Zr and Ti–15Zr–4Nb alloys. The curves show no breakdown potential in any case, which excludes the formation of pits even at high polarisation values. The susceptibility to pitting corrosion is, therefore, very low, and at least comparable to that of other Ti-alloys. The surface analysis exhibits differences on the composition of the passive layer that could have an influence on the passivation current density values observed in the polarisation curves.

Acknowledgements

The authors gratefully acknowledged Professor G. Fommeyer from Max Planck Institut für Eisenforschung (Düsseldorf) for kindly supplying the Ti alloys specimens. This work has been supported by the Project 07N-0050-1999 of the Spanish 'Programa de Tecnología de los Materiales de la Comunidad Autónoma de Madrid'.

References

[1] D.H. Kohn, P. Ducheyne, in: D.F. Williams (Ed.), Medical and Dental Materials, Serie Materials Science and Technology, vol. 14, VCH, Weinheim, 1992 Chapter 2.
[2] H.J. Breme, V. Biehi, J.A. Helsen, in: J.A. Helsen, H.J. Breme (Eds.), Metals as Biomaterials, Wiley, Chichester, 1998 Chapter 2.
[3] J.B. Park, in: J.D. Bronzino (Ed.), The Biomedical Engineering Handbook, CRC Press, FL, USA, 1995 Chapter 40.
[4] D.A. Jones, Principles and Prevention of Corrosion, Prentice Hall, NJ, USA, 1996.
[5] D. Talbot, J. Talbot, Corrosion Science and Technology, CRC Press, Boston, 1998.
[6] J. Cordero, L. Munuera, M.D. Folgueira, J. Bone Jt. Surg. 76 (1994) 717.
[7] C. Lyth, Aust. Corr. Eng. 25 (1970) 34.
[8] A.C. Fraker, A.W. Ruff, J. Metals 5 (1977) 22.
[9] H. Sibum, V. Güther, O. Roidl, in: F. Habashi (Ed.), Alloys, Wiley-VCH, Weinheim, 1998 Chapter 11.
[10] R. Boyer, G. Welsch, E.E. Collings, Materials Properties Handbook: Titanium Alloys, ASM International, 1994.
[11] I. Milosev, M. Metikos-Hukovic, H.H. Strehblow, Biomaterials 21 (2000) 2103.
[12] M. Cabrini, A. Cigada, G. Rondelli, B. Vicentini, Biomaterials 18 (1997) 783.
[13] C. Bathias, K. El Alami K, T.Y. Wu, Eng. Fract. Mech. 56 (1997) 255.
[14] M. Shirkhanzadeh, J. Mater. Sci. Mater. Med. 6 (1995) 206.
[15] S.G. Steinemann, in: G.D. Winter, J.L. Leray, K. De Groot (Eds.), Evaluation of Biomaterials, Wiley, New York, 1980.
[16] Y. Okazaki, S. Rao, Y. Ito Y, T. Tateishi, Biomaterials 19 (1998) 1197.
[17] M. Stern, A.L. Geary, J. Electrochem. Soc. 104 (1957) 56.
[18] M.L. Escudero, M.F. López, J. Ruiz, M.C. García-Alonso, H. Canahua, J. Biomed. Mater. Res. 31 (1996) 313.
[19] M.F. López, A. Gutiérrez, J.A. Jiménez, Surf. Sci. 482 (2001) 300.